

The signal-to-noise problem, well illustrated in Fig. 2, is currently being studied in an attempt to search for fine structure in the absorption edge.

The authors would like to thank those many persons who have lent us encouragement, advice, and equipment.

†This work was supported in part by the National Science Foundation.

\*Alfred P. Sloan Foundation Fellow.

†National Science Foundation Postdoctoral Fellow.

<sup>1</sup>W. Kaiser and C. G. B. Garrett, Phys. Rev. Letters **7**, 229 (1961).

<sup>2</sup>D. A. Kleinman, Phys. Rev. **125**, 87 (1962).

<sup>3</sup>R. Braunstein, Phys. Rev. **125**, 475 (1962).

<sup>4</sup>A. W. Overhauser, Phys. Rev. **101**, 1702 (1956);

D. L. Dexter, Phys. Rev. **108**, 707 (1957); R. S.

Knox and N. Inchauspé, Phys. Rev. **116**, 1093 (1959);

F. Fischer, Z. Physik **160**, 194 (1960).

<sup>5</sup>K. Teegarden, Phys. Rev. **108**, 660 (1957).

<sup>6</sup>F. Fischer and R. Hilsch, Nachr. Akad. Wiss. Göttingen, IIA. Math. Physik. Kl. No. 8, 241 (1959).

## DISTURBANCE OF PHONON DISTRIBUTION IN HIGH ELECTRIC FIELDS

A. Zylbersztejn and E. M. Conwell\*

Laboratoire De Physique De L'Ecole Normale Supérieure, Paris, France

(Received 8 August 1963)

The rate of phonon generation may be calculated from the well-known expressions for the rates of scattering of electrons with phonon emission and absorption, respectively.<sup>1</sup> For the conditions of interest, electron energy is too low for optical phonon emission, and carrier concentration is fairly high. We may therefore take for the distribution function of the electrons in the  $i$ th valley a Maxwell-Boltzmann distribution  $f^{(i)} = \{n/N_c(T_e^{(i)})\} \exp[-\epsilon/k_0 T_e^{(i)}]$ , where  $N_c(T_e^{(i)})$  is the "effective density of states" in the  $i$ th valley. We shall neglect the asymmetric part of the electron distribution and of the disturbed phonon distribution since these are expected to be small. When the phonon disturbance is not too large, the phonon lifetime should be given by the boundary scattering value  $L/u_\alpha$ , where  $u_\alpha$  is the appropriate sound velocity. Taking the steady-state value  $N_q$  of phonons with wave vector  $q$  as the product of the generation rate and this lifetime, we find for  $\hbar u_\alpha q \ll k_0 T_e^{(i)}$

$$N_{q\alpha} = \left[ \sum_{i=1}^g F_\alpha^{(i)} \right] / \left[ 1 + \sum_{i=1}^g F_\alpha^{(i)} \hbar u_\alpha q / k_0 T_e^{(i)} \right], \quad (1)$$

where  $g$  is the number of valleys, and

$$F_\alpha^{(i)} = \frac{1}{2} L \frac{m_t^{3/2} m_l^{1/2}}{\pi \hbar^4 \rho u_\alpha^2} \frac{n^{(i)}}{N_c(T_e^{(i)})} k_0 T_e^{(i)} \frac{\Xi_\alpha^2}{C^{1/2}(\theta_i)} \times \exp\{-[\hbar^2 q^2 / 8mk_0 T_e^{(i)}] C(\theta_i)\}, \quad (2)$$

$$C(\theta_i) = \sin^2 \theta_i + (m_t/m_l) \cos^2 \theta_i, \quad (3)$$

$\theta_i$  being the angle between  $\vec{q}$  and the symmetry axis of the  $i$ th valley. For longitudinal waves  $\alpha = l$  and  $\Xi_l = \Xi_d + \Xi_u \cos^2 \theta_i$ ; for transverse waves  $\alpha = t$  and  $\Xi_t = \Xi_u \sin \theta_i \cos \theta_i$ , the  $\Xi$ 's being the deformation potential constants defined by Herring and Vogt.<sup>1</sup> It is seen that, for the  $F_\alpha^{(i)}$  not large compared to unity, which we shall assume to be the case throughout this treatment, (1) is not in a form for which we may say the phonon distribution has a new temperature.

$N_{ql}$  and  $N_{qt}$  were calculated for  $n$ -Ge, for several directions of  $q$ , with current assumed in the [100] direction, in which case  $T_e^{(i)}$  is the same for all valleys.  $T_e$  was taken as  $10T_{lat}$ , or  $40^\circ$ , and  $\hbar \omega_q / k_0 T_{lat}$  was taken as 2. For  $q$  in the [100] direction, it was found that  $F_t^{(i)} = 3.32nL/5 \times 10^{14}$  for  $L$  in cm,  $n$  in  $\text{cm}^{-3}$ .  $F_l^{(i)}$  for this direction was quite small. For  $q$  in the [111] direction,  $F_l^{(111)} = 12.1nL/5 \times 10^{14}$ , but it is much smaller for the other three valleys. The corresponding quantity for transverse waves is 0 for the [111] valley, and small for the other three valleys. Despite the large anisotropy of  $N_{ql}$  and  $N_{qt}$  individually, their sum has small anisotropy. For  $L = 1$  cm,  $n = 5 \times 10^{14}/\text{cm}^3$ , the sum is  $\approx 4$  for  $q$  in the [100] direction, 5.5 for  $q$  in the [111] direction.

With  $N_q$  given above, one may calculate from the usual formalism<sup>1</sup> the relaxation-time tensor and the mobility, which is a scalar for current in the [100] direction, as functions of  $T_e$ . In turn,  $T_e$  may be determined by the familiar technique

of equating the average rate of energy gain from the field,  $euE^2$ , to the average rate of loss to phonons. In the limit of large  $T_e$ , we find for the latter

$$\left\langle \frac{d\epsilon}{dt} \right\rangle = \frac{8\sqrt{2}}{3\pi^{3/2}} \frac{m_t^2 m_l^{1/2}}{\rho \hbar^4} \left[ 2\Xi_d^2 + \frac{m_l}{m_t} (\Xi_u + \Xi_d)^2 \right] k_0 T_e^{3/2}. \quad (4)$$

Using  $T_e$  determined from the balance-of-energy condition, we find

$$\mu = \Phi(nL)^{-3/4} E^{-1/2}, \quad (5)$$

where  $\Phi$  is a complicated function that increases weakly with increasing  $F_\alpha^{(i)}$ . If there were no departure from the thermal equilibrium phonon distribution, theory predicts<sup>2</sup>  $\mu \propto E^{-0.8}$ , and independent of  $n$  and  $L$ , of course.

To test the theory, measurements of  $j$  vs  $E$  at 4°K were made on a set of As-doped Ge samples whose properties are listed in Table I. The first sample had a square cross section with  $L = 0.97$  cm, and a length of 2 cm. All later samples were made by cutting this sample so as to reduce the cross section while keeping the length constant. Ohmic contacts ( $n^+ - n$  alloyed) were provided at the end faces. For the smallest sample, measurements were also made with side probes. No difference was found, within experimental error, between chemically etched and sandblasted samples, indicating that the boundary scattering was essentially diffuse in the etched specimens. The samples were immersed directly in the liquid helium. The voltage was applied in square pulses of 2 microseconds duration, manually triggered to avoid heating the sample. Changing the repetition rate as well as the pulse length ensured that the sample was always in isothermal conditions.

Table I. Properties of samples.

Cross-sectional dimensions (cm)	Room-temperature mean resistivity (ohm-cm)	$N_D - N_A$ ( $10^{14} \text{ cm}^{-3}$ )
$L = 0.97$	3.7	4.7
$L_1 = 0.95$ $L_2 = 0.43$	4	4.34
$L = 0.42$	3.3	5.26
$L = 0.145$	3.5	4.96

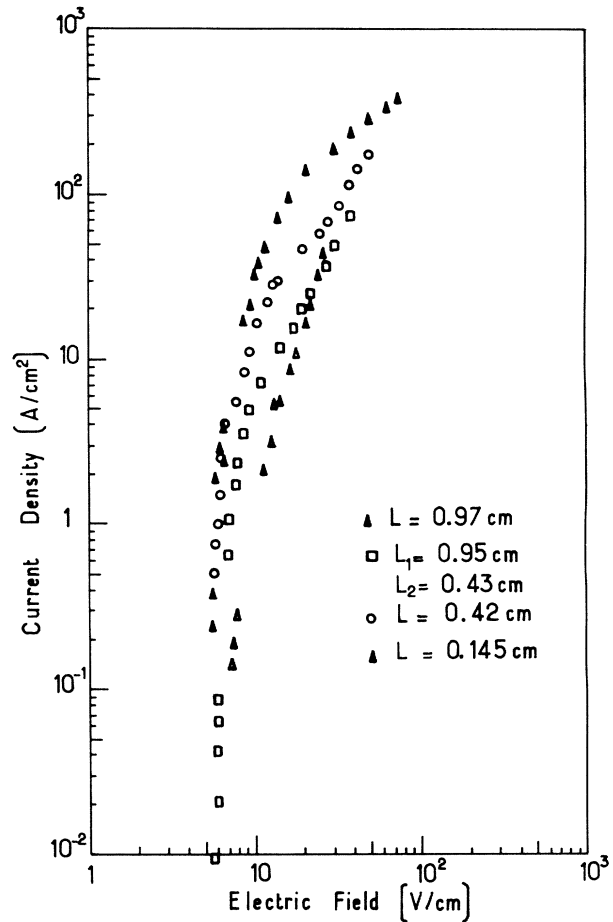


FIG. 1. Current density vs electric field intensity at 4°K for a set of  $n$ -Ge samples with transverse dimensions indicated. All samples had square cross section except for the second, for which the two transverse dimensions are listed.

As is seen in Fig. 1, at low current densities  $j$  vs  $E$  was found to be the same for all samples, indicating that such differences as there are in impurity content and inhomogeneity have no effect. At higher current, or, more significantly, carrier densities, the  $j$  vs  $E$  curves of the different samples are found to fall below the main curve, the deviation coming at a lower carrier density the larger the sample. These are just the effects expected for a disturbance of the phonon distribution. When sufficient phonons are generated, i.e.,  $N_q$  is comparable to  $\frac{1}{2}$ , the additional scattering decreases the rate of energy gain from the field, and thus the electron temperature and, in this range of fields, the electron concentration, which causes lower current for a given field. The effect begins at lower  $n$

in samples of larger  $L$  because  $N_q \propto nL$ . We have estimated the values of  $n$  at which the deviation begins for the different samples and they are in reasonable agreement with the theory.

For the smallest sample, the values of the  $F_\alpha^{(i)}$  are in the range for which the calculations carried out above apply. At the very highest fields it is found that  $j$  varies essentially as  $E^{0.5}$ . Since saturation should certainly have been obtained by these fields, this indicates that  $\mu$  decreases essentially as  $E^{-0.5}$ , in agreement with the theory. Variation of  $\mu$  as  $E^{-0.5}$  under similar experimental conditions has been found previously for both  $n$ -Ge<sup>3</sup> and  $p$ -Ge.<sup>4</sup>

To test the predicted dependence of  $\mu$  on  $L$  we note that at 50 V/cm, the ratio of current densities of the two smallest samples is 1.7, while the  $-\frac{3}{4}$  power of the ratio of their transverse dimensions is 2.2. This is in reasonable agreement with the theory, particularly since for the larger of the two samples the  $F_\alpha^{(i)}$  are large enough so that the dependence of  $\Phi$  on  $L$  has

some effect.

We are grateful to Mr. Menoret of the Centre National D'Etudes des Telecommunications for providing the crystal, and to Mr. Lombard and Mr. Laroche for technical assistance.

\*On leave from General Telephone & Electronics Laboratories, Bayside, New York.

<sup>1</sup>C. Herring and E. Vogt, Phys. Rev. **101**, 944 (1956).

<sup>2</sup>B. V. Paranjape, Proc. Phys. Soc. (London) **B70**, 628 (1959). See also E. M. Conwell and A. L. Brown, J. Phys. Chem. Solids **15**, 208 (1960).

<sup>3</sup>Seymour H. Koenig, Rodney D. Brown, III, and Walter Schillinger, Phys. Rev. **128**, 1668 (1962). Note, however, that Koenig has interpreted these results as indicating that equipartition is valid for the phonons involved, which would also lead to  $\mu$  varying as  $E^{-0.5}$ . Under thermal equilibrium conditions  $N_q$  would be essentially zero for these phonons.

<sup>4</sup>B. M. Vul and E. I. Zavarickaya, Proceedings of the International Conference on Semiconductor Physics, Prague, 1960 (Czechoslovakian Academy of Sciences, Prague, 1961), p. 107.

## TWO-STEP RAMAN SCATTERING IN NITROBENZENE

H. J. Zeiger, P. E. Tannenwald, S. Kern, and R. Herendeen\*

Lincoln Laboratory,<sup>†</sup> Massachusetts Institute of Technology, Lexington, Massachusetts

(Received 9 October 1963)

We have observed emission as a function of angle of coherent Stokes and anti-Stokes radiation from the nitrobenzene in the Kerr cell shutter of a Q-switched ruby laser. Careful measurements of the angular distribution of the three Stokes lines ( $S_1$ ,  $S_2$ , and  $S_3$ ) and one anti-Stokes line ( $AS_1$ ) have allowed a clear-cut distinction between two possible mechanisms that could produce coherent anti-Stokes radiation—namely, a four-photon process and a two-step Raman scattering process. Our data can be explained in terms of the two-step Raman scattering process and is inconsistent with the four-photon model.

In the four-photon process, two laser quanta are annihilated with the emission of a phase-matched Stokes and anti-Stokes quantum. In the two-step Raman scattering process, the laser parametrically stimulates the emission of a distribution of Raman Stokes quanta and associated distributed optical phonons; this is followed by a secondary anti-Stokes Raman scattering process, the annihilation of both laser radiation and the appropriate optical phonons to create phase-matched anti-Stokes radiation. The first of these processes

has been suggested by Terhune<sup>1</sup> to explain his observation of anti-Stokes rings in Raman scattering. The importance of the excitations of optical phonons in stimulated Raman emission was suggested by two of the authors<sup>2</sup>; and the two-step process for the creation of anti-Stokes radiation has been considered within the framework of a formalism similar to the optical-phonon picture.<sup>3</sup>

In our arrangement the sample is simply the nitrobenzene in the Kerr cell shutter of a standard Q-switched ruby laser with an external reflector. This contrasts with the earlier observation of Terhune, who focused the the primary laser beam on an external sample cell. The experiment consists of measurement of the angular distribution of three Stokes and one anti-Stokes lines that were observable with our system. The angular distribution results, obtained with a spectrometer and photomultiplier detector, are shown in Fig. 1. The significant features of the data are these:

(1) The first Stokes line ( $S_1$ ) peaks up in the forward direction, and shows no other major peaks as a function of angle.

(2) The first anti-Stokes line ( $AS_1$ ) does not